Measurement of $\Xi^-/\bar{\Xi}^+$ production in jets from Z boson decays using DELPHI open data*

Zhouyue Fan (范周越)[1,2] Yuzhi Che (车逾之)[1,3†] Xinchou Lou (娄辛丑)[1,2,4] Zhaoru Zhang (张照茹)[1]
Jinfei Wu (吴金飞)[1] Gengyuan Zhang (张耕源)[1,2] Gang Li (李刚)[1,2] Yanping Huang (黄燕萍)[1,2]
Manqi Ruan (阮曼奇)[1,2]

[1]Institute of High Energy Physics, Chinese Academy of Sciences, Beijing 100049, China
[2]University of Chinese Academy of Sciences, Chinese Academy of Sciences, Beijing 100049, China
[3]China Center of Advanced Science and Technology, Beijing 100045, China
[4]Nanjing University, Nanjing 210093, China

Abstract: The production rates of $\Xi^-/\bar{\Xi}^+$ baryons in energy-ranked jets produced from $Z\to$ hadrons decays are measured using 3.2 million hadronic Z decay events recorded by the DELPHI experiment. Jets are reconstructed using the Durham algorithm with $y_{\rm cut}=0.005$. Quark- and gluon-enriched jet samples are obtained by ranking the jet energies in three-jet events. The softest jet is found to produce fewer $\Xi^-/\bar{\Xi}^+$ and less energetic baryons than the other jets. The ratio of $\Xi^-/\bar{\Xi}^+$ production rates in gluon and quark jets, each normalized to the corresponding mean charged-particle multiplicity, is measured to be 1.21 ± 0.18 (stat.) ±0.26 (syst.). This result is consistent with the JETSET expectation and the OPAL measurements of K^0_S and Λ productions in Z decays. This study presents the first measurement of the gluon-to-quark production ratio for baryons containing two s quarks, providing new insights into strange-quark production and hadronization. Future e^+e^- colliders such as CEPC and FCCee will provide much larger Z-boson samples and enable far more precise studies of the subject.

Keywords: hadronization, QCD, baryons

DOI: 10.1088/1674-1137/aea82b **CSTR:**

I. INTRODUCTION

Quantum chromodynamics (QCD) theory predictions suggest that gluon jets will exhibit stronger color radiation in the perturbative parton cascade and contain larger particle multiplicities [1, 2] in hadronic Z decays. This general enhancement is largely reflected in inclusive charged-particle production. For the identified hadron species, the observed differences between quark and gluon jets also encode properties of non-perturbative QCD. Earlier studies investigated K^0_S and Λ production in energy-ranked jets and derived the ratios of their production rates in gluon and quark jets relative to the mean charged-particle multiplicity,

$$\mathcal{R}^h_{g/q}\equiv\frac{\langle N_h\rangle_g}{\langle N_{\rm ch}\rangle_g}\Big/\frac{\langle N_h\rangle_q}{\langle N_{\rm ch}\rangle_q}, \tag{1}$$

where $\langle N_h\rangle_g$ and $\langle N_h\rangle_q$ are the average yields of hadron type h in gluon and quark jets, respectively, while $\langle N_{\rm ch}\rangle_g$ and $\langle N_{\rm ch}\rangle_q$ represent the mean charged-particle multiplicities in gluon and quark jets. The results showed that the identified strange-hadron production in gluon jets cannot be fully explained through a general scaling of inclusive charged-particle multiplicity in gluon jets [3]. Furthermore, measurements of single-strange baryon–antibaryon correlations indicate that baryon-number and strangeness compensation in QCD depend on the baryon species and rapidity separation [4–6]. In this context, the production of doubly-strange baryons, Ξ^-, in jets intrinsically involves both strange hadron production and local compensation of baryon number, thereby making it a sensitive probe of non-perturbative QCD. The production of Ξ^- baryons has been experimentally investigated in inclusive Z decays by OPAL [7, 8] and DELPHI [9, 10]; however, its dependence on the jet environment remains

Received 31 July 2026; Accepted 14 September 2026; Accepted manuscript online 15 September 2026

* Supported by the National Natural Science Foundation of China (12342502). This paper is also supported by the Xiejialin Fund (E65461U2), the Innovation Fund of IHEP (E65451U8) and the Start-up Fund of IHEP (E55156U1)

† E-mail: cheyuzhi@ihep.ac.cn

Content from this work may be used under the terms of the Creative Commons Attribution 3.0 licence. Any further distribution of this work must maintain attribution to the author(s) and the title of the work, journal citation and DOI. Article funded by SCOAP[3] and published under licence by Chinese Physical Society and the Institute of High Energy Physics of the Chinese Academy of Sciences and the Institute of Modern Physics of the Chinese Academy of Sciences and IOP Publishing Ltd

unexplored. Three-jet hadronic Z events provide experimentally accessible quark- and gluon-enriched jet samples, enabling a differential study of Ξ^- production in distinct jet categories.

In 2024, the DELPHI data set and the full simulation and reconstruction software stack were released to the global high-energy-physics community [11], enabling further investigations of the strange-baryon production in Z decays.

This paper reports a measurement of $\Xi^-/\bar{\Xi}^+$ production in two- and three-jet events using DELPHI data collected during 1992–1995. The production rates are reported as functions of jet energy and jet energy rank. The $\xi = -\ln(p_\Xi/E_{\rm beam})$ spectra are compared among energy-ranked jet samples. For three-jet events, the generator-modeled gluon fractions of the energy-ranked jets are used to infer the ratio of $\Xi^-/\bar{\Xi}^+$ production rates per mean charged-particle multiplicity in gluon and quark jets, $\mathcal{R}^{\Xi^-}_{g/q}$.

The rest of this paper is organized as follows. Section II summarizes the DELPHI detector, open data samples, and corresponding simulated samples used in the analysis. Section III describes the jet reconstruction, energy-ranked jet classification, generator-level gluon-fraction estimate, and reconstruction and selection of $\Xi^-/\bar{\Xi}^+$ candidates. The $\Xi^-/\bar{\Xi}^+$ yield extraction, efficiency correction, uncertainty evaluation, and the resulting measurements in energy-ranked jets are presented in Section IV. The main findings are summarized in the final section. Unless stated otherwise, Ξ^- represents the sum of Ξ^- and its charge-conjugate state $\bar{\Xi}^+$.

II. DELPHI DETECTOR, DATA, AND SIMULATION SAMPLES

The DELPHI detector and its performance are described in detail in Refs. [12, 13]. From the beam pipe outwards, the central detector included the vertex detector (VD), inner detector, time projection chamber, outer detector, ring imaging Cherenkov counter, high-density projection chamber electromagnetic calorimeter, hadron calorimeter instrumented in the iron return yoke, and barrel muon chambers. The entire tracking system operated inside a magnetic field of 1.2 T, parallel to the beam axis. During the 1991–1993 running period, the VD included three layers of single-sided silicon microstrip detectors at radii of approximately 6.3, 9, and 11 cm; from 1994 onward, the use of double-sided silicon detectors enabled three-dimensional impact-parameter reconstruction, improving secondary-vertex reconstruction and heavy-flavor tagging [13].

This study uses the Z-decay data collected in 1992–1995. The sample nicknames and digital object identifiers (DOIs) are listed in Table 1. The corresponding Monte Carlo (MC) samples of inclusive $e^+e^- \to Z \to q\bar{q}$ events, produced with the DELPHI built-in generator [14] and released with the data set, are used to interpret the data and estimate the selection efficiency for Ξ^- candidates. These samples are also listed in Table 1 and are stored in the original DELPHI DST data format. A dedicated tool, adapted from the software described in Ref. [15], is used to extract the information relevant to the analysis from the DST files and to store it in ROOT files [16].

Table 1. Nicknames and digital object identifiers (DOIs) of the data sets and official simulation samples used in this analysis.

Type	Year	Sample	DOI
Data	1992	short92_e2	[17]
Data	1993	short93_d2	[18]
Data	1994	short94_c2	[19]
Data	1995	short95_d2	[20]
MC	1992	sh_kk2f4146qqpy_e91.25_c92_2l_e2	[21]
MC	1993	sh_kk2f4146qqpy_e91.25_c93_2l_d2	[22]
MC	1994	sh_kk2f4146qqpy_e91.25_l94_2l_c2	[23]
MC	1995	sh_kk2f4146qqpy_e91.25_c95_1l_d2	[24]

All events are required to pass the official "Team 4" selection encoded in the open data as a tag, after which approximately 3.23×10^6 events remain. In each event, reconstructed particles are selected according to official criteria [13, 25].

III. JET CLUSTERING AND Ξ^- RECONSTRUCTION

To investigate Ξ^- production in jets, the e^+e^- $k_\perp$ clustering algorithm, referred to as the Durham algorithm [26], is implemented using the $\rm F_{ASTJET}$ [27] package. All charged and neutral reconstructed particles satisfying the requirements described in Section II are used as jet-clustering inputs. In the Durham algorithm, the distance between input objects i and j is defined as

$$y_{ij} = \frac{2\min(E_i^2, E_j^2)(1-\cos\theta_{ij})}{Q^2}, \tag{2}$$

where E_i and E_j are the object energies, Q is the center-of-mass energy, and θ_{ij} is the opening angle between the two objects. Following Ref. [3], the jet resolution parameter is set to $y_{\rm cut} = 0.005$.

The jet energy is defined as the sum of the energies of the reconstructed particles assigned to the jet, with charged particles treated as pions and neutral particles treated as photons. In two- and three-jet events, the reconstructed jets are ordered by energy and labeled the most energetic jet (***Jet 1***), second-most energetic jet (***Jet 2***), and third-most energetic jet (***Jet 3***).

The gluon fraction of each energy-ranked jet cat-

egory is estimated from the MC samples using generator-level parton information. A list of generator-level reference partons is constructed from the primary partons whose parent is the generated Z boson. The most energetic generated gluon in the event is included. The reconstructed jets are matched to the generator-level partons based on the smallest angular separation between their momentum directions. The gluon fraction is defined as the fraction of jets in the category that are matched to a gluon. The resulting average gluon fractions of ***Jet 1***, ***Jet 2***, and ***Jet 3*** are 10.3%, 26.3%, and 63.2%, respectively.

The Ξ^- candidates are reconstructed via the cascade decay $\Xi^- \to \Lambda\pi^-$, followed by $\Lambda \to p\pi^-$. Λ candidates are reconstructed from oppositely charged particle pairs (V^0 candidates) originating from decays in the flights of neutral particles, using the standard DELPHI V^0 algorithm [13]. All V^0 candidates are treated as Λ candidates and combined with additional charged tracks to form Ξ^- cascade decays. An external package for vertex fitting [28] is used to reconstruct the two vertices in the Ξ^- cascade. The higher-momentum daughter track of the Λ candidate is assigned the proton mass, while the other daughter is assigned the pion mass. The momenta of the three charged daughter tracks are corrected using the corresponding Ξ^- and Λ decay vertices as their points of origin.

For Ξ^- candidate selection, the two pion tracks are required to have the same charge. The Λ candidates must satisfy $|m_\Lambda - 1116.3\ \text{MeV}| < 4.5\ \text{MeV}$. The χ^2 probabilities for both constraints in the $\Xi^- \to \Lambda\pi^-$ vertex fit need to be greater than 0.1%. To further suppress combinatorial background, the signed decay radius of each Ξ^- candidate in the $R\phi$ plane must satisfy

$$R_\Xi = \left\{ \begin{array}{lll} +r_\Xi & \text{if} & r_\Lambda > r_\Xi, \\ -r_\Xi & \text{if} & r_\Lambda \le r_\Xi, \end{array} \right\} > 0.4\,\text{cm}, \tag{3}$$

where r_Ξ and r_Λ are the transverse distances of the $\Xi^- \to \Lambda\pi^-$ and $\Lambda \to p\pi^-$ decay vertices from the beam spot, respectively. The DELPHI detector has limited acceptance for Ξ^- baryons outside the range $1.0 < \xi \equiv -\ln(p_\Xi/E_\text{beam}) < 4.0$; consequently, only candidates within this range are used in this analysis. The resulting invariant-mass spectrum of the Ξ^- candidates in all Z-decay events is shown in Fig. 1.[1)]

Each reconstructed $\Xi^-/\bar{\Xi}^+$ candidate is assigned to a jet according to its distance from the reconstructed jets. The quantity $y_{\Xi\text{jet}}$, defined in Eq. (2), is calculated using the four-momenta of each Ξ^- candidate and jet. If the minimum value of $y_{\Xi\text{jet}}$ for a given Ξ^- candidate is smaller than y_cut, the candidate is assigned to the corresponding jet.

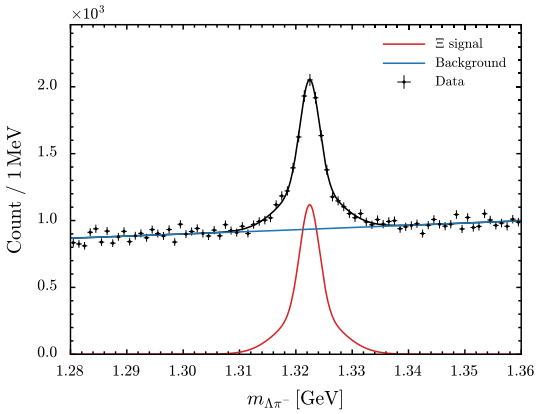


Fig. 1. (color online) Invariant mass distribution of the selected Ξ^- candidates from all data samples listed in Table 1. The spectrum is fitted with a double-Gaussian function (red curve) and a third-order polynomial function (blue curve).

IV. AVERAGE Ξ^- PRODUCTION IN ENERGY-RANKED JETS

This analysis begins with the selection of hadronic events. All jets in each event must have polar angles in the range $30° < \theta_\text{jet} < 150°$.

Jets in the 2- and 3-jet events are grouped into bins of reconstructed jet energy. The average Ξ^- production per jet is calculated as

$$\langle N_\Xi \rangle = \frac{1}{N_{\text{jet},k}} \frac{N^{\Xi^-}_{\text{obs},k}}{\epsilon_k f_{\text{acc},k}}, \tag{4}$$

where $N_{\text{jet},k}$ represents the number of reconstructed jets included in the Ξ^- production measurement. The number of observed Ξ^- candidates ($N_{\text{obs},k}$) is obtained from fits to the Ξ^- mass spectra in the corresponding jets. The quantities ϵ_k and $f_{\text{acc},k}$ are the selection efficiency and acceptance factor, respectively, estimated from the MC samples.

When fitting the Ξ^- mass spectrum, the signal probability density function is modeled using kernel density estimation (KDE) with a Gaussian kernel based on the MC simulation. The KDE bandwidth follows the adaptive prescription of Ref. [29]. The combinatorial background is modeled using wrong-sign control candidates. These candidates are formed from $\Lambda\pi^+$ and $\bar{\Lambda}\pi^-$ combinations and passed through the same reconstruction procedure and selection requirements as the right-sign Ξ^- candidates. The wrong-sign candidates are then used to

1) Because the magnetic-field conditions are not fully known, the Ξ^- candidate mass distributions are biased. Following the calibration used in the official study [10], a residual mass-scale correction is applied to the Ξ^- mass in data. The correction is calibrated using the mass shifts of Λ and K_S^0 candidates, and the distribution in the MC samples is artificially shifted to match the nominal Ξ^- mass.

construct the background KDE template. The obtained signal yields are used as raw inputs for data correction.

The ϵ_k and $f_{\mathrm{acc},k}$ in Eq. (4) are estimated using MC simulations. In the MC samples, the generated Ξ^- baryons are assigned to jets using the same Durham-distance criterion as that utilized in the jet-clustering algorithm. The generated Ξ^- baryons are then matched to the reconstructed Ξ^- candidates using MC information. For each energy-ranked jet, the efficiency ϵ_k is defined as the ratio of the selected Ξ^- candidates matched to truth Ξ^- baryons to the total number of generated truth Ξ^- baryons. The acceptance factor $f_{\mathrm{acc},k}$ is defined as the ratio of the generated Ξ^- baryons within $1.0 < \xi < 4.0$ to all generated Ξ^- baryons assigned to the corresponding jet category.

Uncertainties The statistical uncertainty includes contributions from the fitted signal yield in data and the finite MC statistics utilized in the efficiency and acceptance correction. These components are propagated through the correction procedure.

The systematic uncertainty from the Ξ^- selection is evaluated by repeating the measurement with varied selection requirements. The m_Λ window is varied from the nominal 4.5 MeV to 4.0 MeV and 5.0 MeV. The requirement on the signed Ξ^- decay radius in the $R\phi$ plane is varied from the nominal 0.4 cm to 0, 0.5 cm, and 2.5 cm. For each source, the largest variation with respect to the nominal result is taken as the corresponding systematic uncertainty.

The systematic uncertainty associated with the signal yield extraction model is estimated with an alternative method. In this procedure, the background in each Ξ^- mass spectrum is modeled with wrong-sign control samples, and its normalization is determined by fitting the spectrum outside a ±10 MeV window around the Ξ^- mass. The signal yield is then obtained by subtracting the normalized background contribution from the data within the ±10 MeV signal window. Half of the difference between this yield and the nominal fit result is assigned as the fit-model systematic uncertainty.

The acceptance factor used to extrapolate from $1.0 < \xi < 4.0$ to the full kinematic range is derived from the JETSET generator and is therefore model dependent. Following the previous study [10], a relative uncertainty of ±50% is assigned to the amount of compensation. The total systematic uncertainty is obtained by adding the individual systematic components in quadrature.

Result Figure 2 shows the average Ξ^- baryon production per jet for energy-ranked jets, and the corresponding values are listed in Table 2. The measurements in the leading and subleading jets are similar in both two- and three-jet events. In three-jet events, the softest jet category yields a lower value. All measurements remain compatible with the JETSET prediction within the uncertainties.

V. MOMENTUM SPECTRA

The $\xi = -\ln(p_\Xi/E_{\mathrm{beam}})$ spectra of the Ξ^- baryons in

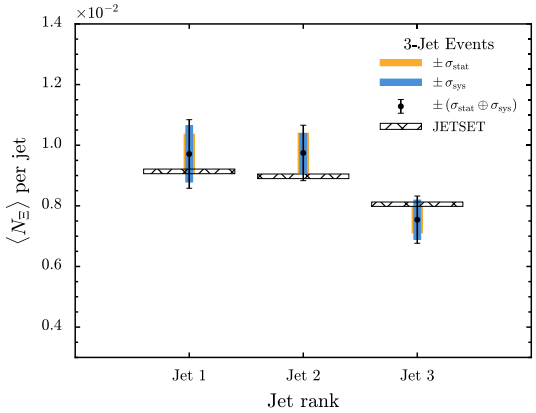


Fig. 2. (color online) Average Ξ^- production per jet in the energy-ranked jets for (left) two- and (right) three-jet events. The measurements are compared with the JETSET prediction.

Table 2. Average Ξ production per jet in the two- and three-jet events. The central observable is computed as $\langle N_\Xi \rangle = N_{\mathrm{obs}}/(\epsilon f_{\mathrm{acc}} N_{\mathrm{jet}})$ from the fitted signal yield (N_{obs}), selection efficiency (ϵ), acceptance factor (f_{acc}), and number of jets (N_{jet}). Relative statistical (σ_{stat}) and systematic ($\sigma^{\mathrm{tot}}_{\mathrm{syst}}$) uncertainties in $\langle N_\Xi \rangle$ are listed as percentages. The total systematic uncertainty $\sigma^{\mathrm{tot}}_{\mathrm{syst}}$ is decomposed into contributions from the Λ-mass selection (Δm_Λ), signed Ξ^- decay radius in the $R\phi$ plane (R_Ξ), method used to extract the signal yield (Fit), and acceptance correction (Acc.). The individual uncertainties are added in quadrature to obtain the total uncertainty (σ_{total}) listed in the last column.

Jet Num.	Jet Rank	N_{obs}	ϵ (%)	f_{acc} (%)	N_{jet}	$\langle N_\Xi \rangle \times 10^{-3}$	σ_{stat} (%)	σ_{syst}				σ_{syst} (%)	σ_{total} (%)
								Δm_Λ	R_Ξ	Fit	Acc.		
3-jet	Jet 1	760.5	10.4	84.5	889570	9.71	$^{+6.7}_{-6.7}$	2.9	4.7	0.5	7.8	9.5	$^{+11.7}_{-11.6}$
3-jet	Jet 2	789.4	10.3	88.0	889570	9.74	$^{+6.7}_{-6.7}$	0.5	1.7	2.1	6.0	6.6	$^{+9.4}_{-9.4}$
3-jet	Jet 3	852.0	13.8	92.2	889570	7.54	$^{+5.8}_{-5.7}$	2.8	6.8	2.1	3.9	8.6	$^{+10.3}_{-10.3}$

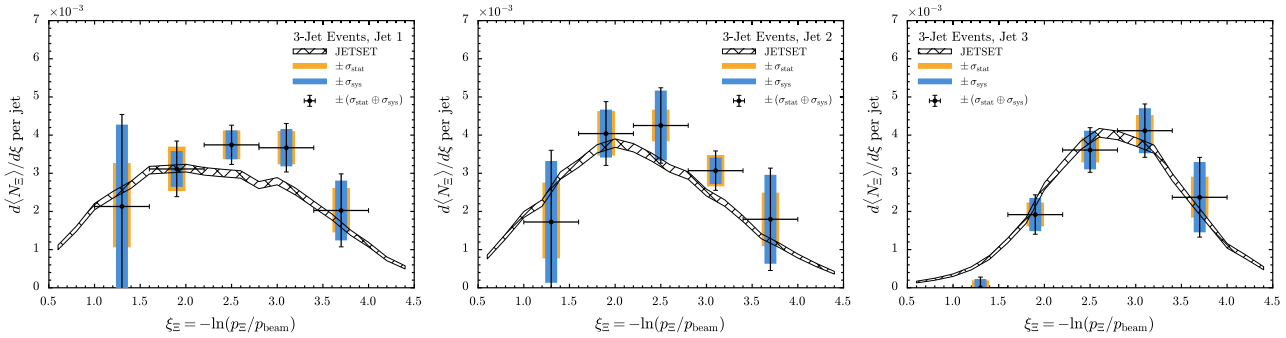


Fig. 3. (color online) Differential Ξ^- production spectra as a function of $\xi_\Xi=-\ln(p_\Xi/p_{\rm beam})$ in ***Jet 1***, ***Jet 2***, and ***Jet 3*** of the three-jet events.

energy-ranked jets are also measured in this study. Within each energy-ranked jet category, the selected Ξ^- candidates are further divided into bins of ξ,

$$\frac{{\rm d}\langle N_\Xi\rangle}{{\rm d}\xi}\simeq\frac{\Delta\langle N_\Xi\rangle}{\Delta\xi}=\frac{1}{\Delta\xi}\frac{1}{N_{\rm jet}}\frac{N_{\rm obs}}{\epsilon}. \tag{5}$$

The efficiency correction and uncertainty estimation follow the procedure described in Section IV. The results are shown in Fig. 3. The average ξ values for the Ξ^- baryons in ***Jet 1***, ***Jet 2***, and ***Jet 3*** are $2.51^{+0.11}_{-0.10}({\rm stat})\pm 0.19({\rm syst})$, $2.33^{+0.10}_{-0.10}({\rm stat})\pm0.16({\rm syst})$, and $2.84^{+0.05}_{-0.05}({\rm stat})\pm 0.082({\rm syst})$, respectively. The momentum of the Ξ^- baryons in ***Jet 3*** tends to be lower than that in ***Jet 1*** and ***Jet 2***. The spectra are consistent with the JETSET prediction.

VI. RELATIVE Ξ^- PRODUCTION AND GLUON-TO-QUARK RATE

Following the methods of previous studies [3, 30], this study determines $\mathcal{R}^{\Xi^-}_{g/q}$, as defined in Eq. (1).

The jet samples are treated as mixtures of gluon and quark jets. For a jet category indexed by k, the observed production rate of an identified particle (h) relative to the production of inclusive charged tracks is expressed as

$$\mathcal{R}^h_k\equiv\frac{\langle N_h\rangle}{\langle N_{\rm ch}\rangle}=\rho_k\cdot\mathcal{R}_g+(1-\rho_k)\cdot\mathcal{R}_q, \tag{6}$$

where $\langle N_h\rangle$ is the average yield of the particle per jet, $\langle N_{\rm ch}\rangle$ represents the average yield of inclusive charged tracks, and ρ_k is the gluon fraction of the jet category. The $\mathcal{R}_q$ and $\mathcal{R}_g$ are the relative production rates of the particle in quark and gluon jets, respectively. $\mathcal{R}_g$ and $\mathcal{R}_q$ can be obtained by minimizing

$$\chi^2=\left(\mathbf{R}^h-A\boldsymbol{\theta}\right)^T V^{-1}\left(\mathbf{R}^h-A\boldsymbol{\theta}\right), \tag{7}$$

where V is the covariance of $\mathbf{R}^h$. The ratio of the production rates for pure gluon and quark jets may be determined as $\mathcal{R}_{g/q}\equiv\mathcal{R}_g/\mathcal{R}_q$.

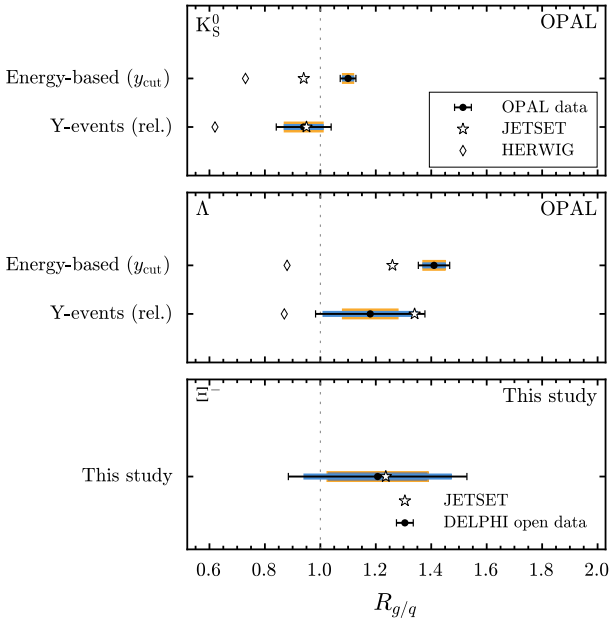


Fig. 4. (color online) Comparison of the gluon-to-quark jet production ratio $\mathcal{R}_{g/q}$ for strange hadrons. The K^0_S and Λ results, along with the JETSET and HERWIG predictions, are obtained from the OPAL measurements [3]. Yellow and blue bands indicate statistical and systematic uncertainties, and black error bars show their quadrature sum.

In this study, $\langle N_{\rm ch}\rangle_k$ is measured in the same events and energy-ranked jet categories as the numerator of $\mathcal{R}^{\Xi^-}_k$. The corresponding reconstruction efficiency is evaluated from simulations as the ratio of reconstructed to generator-level charged-particle yields and used to correct the multiplicity measured in data.

Taking $\langle N_{\rm ch}\rangle_k$ and $\langle N_\Xi\rangle_k$ as inputs, the fit yields an effective gluon-to-quark ratio for Ξ^- production of $\mathcal{R}^{\Xi^-}_{g/q}=1.21\pm0.18\,({\rm stat.})\pm0.26\,({\rm syst.})$. The uncertainties in $\langle N_{\rm ch}\rangle_k$ and $\langle N_\Xi\rangle_k$ are propagated to the fitted ratio, while correlatedsystematicuncertainties in $\langle N_{\rm ch}\rangle_k$ largelycancelout.

The nominal gluon fractions are obtained from the official MC simulation. To estimate the effect of the MC

generator on the $\mathcal{R}_{g/q}^{\Xi^-}$ result, a PYTHIA 8 sample of a sample size comparable to that of the data is used, providing alternative gluon fractions of 10.9%, 24.7%, and 56.1% for the three energy-ranked jet categories, respectively. Repeating the fit with these fractions changes $\mathcal{R}_{g/q}^{\Xi^-}$ by an amount considerably smaller than those of the other uncertainties.

Figure 4 compares this result with the $\mathcal{R}_{g/q}$ values for K_S^0 and Λ production measured by OPAL [3].

VII. CONCLUSION

This work presents the first measurement of the production of doubly strange baryons, $\Xi^-/\bar{\Xi}^+$, in gluon- and quark-enriched jets using three-jet events from hadronic Z boson decays recorded by the DELPHI experiment during 1992–1995. The jets are reconstructed with the Durham algorithm using $y_{\rm cut} = 0.005$ and ordered according to their energies. The lowest-energy jet is enriched in gluon jets, while the two higher-energy jets are enriched in quark jets. The softest jet has lower $\Xi^-/\bar{\Xi}^+$ production rates and softer momentum spectra than those of the other two energy-ranked jets. These results are consistent with the JETSET prediction.

The ratio of $\Xi^-/\bar{\Xi}^+$ production rates in gluon jets to quark jets, each normalized to the corresponding mean charged-particle multiplicity, is determined to be $\mathcal{R}_{g/q}^{\Xi^-}{}_{K_S^0} = 1.21 \pm 0.18\,(\text{stat.}) \pm 0.26\,(\text{syst.})$; this is consistent with $\mathcal{R}_{g/q}^{K_S^0}$ and $\mathcal{R}_{g/q}^{\Lambda}$ reported by OPAL [3]. The $\mathcal{R}_{g/q}^{\Xi^-}$ ratio is consistent with unity within uncertainties, indicating that the enhancement of $\Xi^-/\bar{\Xi}^+$ production in gluon jets relative to quark jets is compatible with that observed for inclusive charged particles. The precision of the present measurement is limited by the available data sample. Future e^+e^- colliders such as CEPC and FCCee operating at the Z pole are expected to provide substantially larger data samples, which will enable more precise studies of the productions of hadrons in gluon and quark jets.

ACKNOWLEDGMENTS

The authors are grateful to the DELPHI Collaboration for the open data which allowed this study to be performed. We thank the BESIII Collaboration and Xiongfei Wang for sharing the analysis code and for their assistance with the vertex-fitting technique. We also thank Hideki Okawa for the valuable suggestions.

References

[1] A. Capella, I. M. Dremin, J. W. Gary *et al.*, Phys. Rev. D **61**, 074009 (2000), arXiv: hep-ph/9910226
[2] S. Bethke, Phys. Rept. **403-404**, 203 (2004), arXiv: hep-ex/0406058
[3] K. Ackerstaff *et al.* (OPAL Collaboration), Eur. Phys. J. C **8**, 241 (1999), arXiv: hep-ex/9805025
[4] G. Abbiendi *et al.* (OPAL Collaboration), Eur. Phys. J. C **13**, 185 (2000), arXiv: hepex/9808031
[5] G. Abbiendi *et al.* (OPAL Collaboration), Eur. Phys. J. C **64**, 609 (2009), arXiv: 0910.2174[hep-ex]
[6] P. Abreu *et al.* (DELPHI Collaboration), Phys. Lett. B **416**, 247 (1998)
[7] P. D. Acton *et al.* (OPAL Collaboration), Phys. Lett. B **291**, 503 (1992)
[8] G. Alexander *et al.* (OPAL Collaboration), Z. Phys. C **73**, 569 (1997)
[9] P. Abreu *et al.* (DELPHI Collaboration), Z. Phys. C **67**, 543 (1995)
[10] J. Abdallah *et al.* (DELPHI Collaboration), Phys. Lett. B **639**, 179 (2006), arXiv: hep-ex/0606030
[11] The DELPHI Collaboration, *Delphi data preservation, reuse, and open access policy*, CERN Open Data Portal (2024)
[12] P. Aarnio *et al.* (DELPHI Collaboration), Nucl. Instrum. Meth. A **303**, 233 (1991)
[13] V. Chabaud *et al.* (DELPHI Collaboration), Nucl. Instrum. Meth. A **368**, 314 (1996)
[14] The DELPHI Collaboration, Creating DELPHI simulated data
[15] J. Zhang *et al.* (Electron-Positron Alliance), *Analysis note: measurement of thrust and track energy-energy correlator in e^+e^- collisions at 91.2 GeV with DELPHI open data* (2025), arXiv: 2510.18762 [hep-ex]
[16] R. Brun and F. Rademakers, Nucl. Instrum. Meth. A **389**, 81 (1997)
[17] The DELPHI Collaboration, DELPHI collision data short92_e2 (2024)
[18] The DELPHI Collaboration, DELPHI collision data short93_d2 (2024).
[19] The DELPHI Collaboration, DELPHI collision data short94_c2 (2024)
[20] The DELPHI Collaboration, DELPHI collision data short95_d2 (2024).
[21] The DELPHI Collaboration, DELPHI simulation data sh_kk2f4146qqpy_e91.25_c92_2l_e2 (2024)
[22] The DELPHI Collaboration, DELPHI simulation data sh_kk2f4146qqpy_e91.25_c93_2l_d2 (2024)
[23] The DELPHI Collaboration, DELPHI simulation data sh_kk2f4146qqpy_e91.25_l94_2l_c2 (2024)
[24] The DELPHI Collaboration, DELPHI simulation data sh_kk2f4146qqpy_e91.25_c95_1l_d2 (2024)
[25] The DELPHI Collaboration, DELPHI skeleton analysis framework manual (2024)
[26] S. Catani, Y. L. Dokshitzer, M. Olsson *et al.*, Phys. Lett. B **269**, 432 (1991)
[27] M. Cacciari, G. P. Salam, and G. Soyez, Eur. Phys. J. C **72**, 1896 (2012), arXiv: 1111.6097[hep-ph]
[28] M. Xu *et al.*, Chin. Phys. C **33**, 428 (2009)
[29] I. S. Abramson, The Annals of Statistics **10**, 1217 (1982)
[30] P. D. Acton *et al.* (OPAL Collaboration), Z. Phys. C **58**, 387 (1993)